J. Min. Metall. Sect. B-Metall. 51 (2) B (2015) 117 - 123

Journal of Mining and Metallurgy, Section B: Metallurgy

SECONDARY LEDEBURITE FORMATION DURING VARIOUS WELDING TECHNIQUES

M.P. Tonkovič [a,*], M. Gojić [b], B. Karpe [c], L. Kosec [c]

[a] High Mechanical Engineering School, Novo mesto, Slovenia
[b] University of Zagreb, Faculty of Metallurgy, Sisak, Croatia
[c] University of Ljubljana, Faculty of Natural Sciences and Engineering, Ljubljana, Slovenia

(Received 16 June 2014; accepted 18 February 2015)

Abstract

The occurrence and formation sequence of secondary ledeburite in the heat affected zone of chromium ledeburitic tool steel W.Nr. 1.2379 (OCR12 VM) after welding with SAW, TIG, microplasma and laser welding techniques is presented in this paper. Special attention was paid on the behaviour of carbides. The occurrence of secondary ledeburite is a result of local enrichment of the austenite matrix with alloying elements, due to partial or complete dissolution of primary/eutectic carbides. The results show that the largest amount of secondary ledeburite is formed during submerged arc welding, followed by TIG and microplasma welding technique. Welding by laser technique, with appropriate technological parameters, could prevent secondary ledeburite formation.

Keywords: Tool steel; Welding techniques; Heat affected zone (HAZ); Carbides; Secondary ledeburite.

1. Introduction

Chromium ledeburitic steels are one of the basic tool steels for cold work processes, where wear resistance is important, such as blanking, die forming, wood cutting, etc. According to chemical composition, W.Nr. 1.2379 steel is classified as high carbon, high chromium steel with vanadium and molybdenum addition. Microstructure depends on the cooling rate and it can be composed of martensite, bainite or pearlite matrix with a larger amount (≈15%) of eutectic (primary ledeburite (γ_{Fe}+M_7C_3)) and secondary carbides. Secondary carbides (M_7C_3, $M_{23}C_6$, M_3C, M_2C, MC) precipitate from the matrix, during slow cooling to room temperature [1-5]. In as cast state, primary ledeburite solidifies in the form of continuous net around matrix grains, which makes this steel extremely fragile. Breaking the eutectic net and attainment of homogeneous distribution of carbides are the main tasks of deformation forming at elevated temperatures. The mechanical properties of the steel are in close correlation with the size, type, morphology, amount and distribution of carbides as well as to the matrix grain size, and could be controlled by the production process parameters. Larger carbides, designated as primary carbides due to their similar morphology, are actually formed through the process of conglomeration and subsequent growth of eutectic carbides during processing at elevated temperatures. Because their limited workability at lower processing temperatures, special attention should be paid to the heating procedure to achieve complete dissolution of secondary carbides in the austenite matrix and to prevent primary (eutectic) carbides and austenite grain growth.

In the processes of intensive heat penetration, such as welding or surface welding (surfacing), diffusion controlled rearrangement of carbon and alloying elements between primary (eutectic), secondary carbides and matrix could occur to such extent that in the surrounding of primary carbides, an area of eutectic chemical composition is reached [6]. If the duration of the adequately high temperature is long enough, this area will locally melt and during cooling solidified into so called secondary eutectic (secondary ledeburite), with typical lamellar structure. The heat affected zone (HAZ) of chromium ledeburitic steels is especially subject to the formation of secondary ledeburite, particularly in the area of partially or completely dissolved larger carbides [7].

Due to different inputs of heat energy during the various welding processes, the width of the HAZ as well as temperature gradients across the HAZ differ [7-10], and so does the amount of secondary ledeburite. It is very substantial after TIG, microplasma or submerged arc welding and very limited or rather undeveloped after laser welding or laser surfacing method. Welding of tool steels is

* *Corresponding author: blaz.karpe@omm.ntf.uni-lj.si*

DOI:10.2298/JMMB140616014T

challenging [11], because they tend to crack [12]. To avoid cracking, they have to be preheated and slowly cooled after welding [13]. The goal of this paper is to show and explain the formation of secondary ledeburite in chromium ledeburitic tool steel W.Nr. 1.2379 (OCR12 VM) after welding and surfacing with various types of welding techniques.

2. Experimental procedure

Specimens for welding and surfacing were prepared by machine treatment of the forged bulk piece of a metal. Base material (A) and three different filler materials (Table 1) were used in the experiment. Filtub dur 112 material (B) was used for submerged arc welding (SAW), 1.4718 steel (C) for TIG surface welding, and Laser - Castolin 60 H material (D) for microplasma surface welding technique.

Surface welds (surfacing) were produced by SAW, TIG, microplasma and laser techniques (Fig. 1a). Welding of V-joint was made only by SAW technique. The SAW welding pass sequence was carried out in three steps (Fig.1b): first weld layer (1), followed by welding the weld face (2), and final welding of the weld root (3). The temperature of the preheating for surface welding by TIG and microplasma technique was 400 °C. For SAW and laser welding, preheating of the steel was not applied. The analysis and characterization of microstructure after welding or surfacing were carried out by optical microscopy (OM) and scanning electronic microscopy (SEM) with corresponding energy dispersive spectrometry methods (EDXS).

Table 1. *Chemical composition of steel (base material) and filler material.*

	Chemical composition / wt. %							
	C	Si	Mn	P	S	Cr	Mo	V
A	1.5	0.4	0.4	0.03	0.03	11.5	0.8	0.85
B	0.08	0.35	1.4	/	0.03	5	0.85	/
C	0.5	2.9	0.8	0.04	0.03	9	/	/
D	1	0.4	0.3	/	/	4	9	2

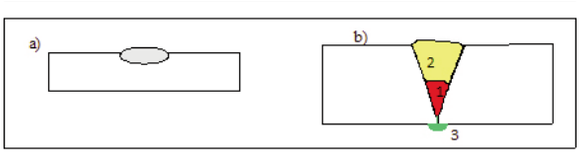

Figure 1. *Schematic illustration of specimens for: a) surfacing, b)V-joint welding pass sequence.*

3. Results

Microstructure of characteristic areas of the weld joint, produced by SAW technique, is shown in Fig. 2. The average HAZ width was 2 mm. On the interface with the weld metal, secondary ledeburite in the HAZ (Fig. 2b) is visible. Secondary ledeburite has a multi-component chemical composition (Table 2, Fig. 2b, Fig. 3), which vary with the position of its formation.

Microstructure of distinctive areas of the surface

Table 2. *Chemical composition of secondary ledeburite (without carbon).*

Place of analysis	Chemical composition / wt.%				
	Fe	Si	Cr	V	Mo
HAZ: cold / hot part	68.1	0.18	27.4	3.03	0.82
HAZ: hot part - place 1	66.4	0.08	28.4	1.5	3.7
HAZ: hot part / weld	64.5	0.13	29.7	3.6	2.02

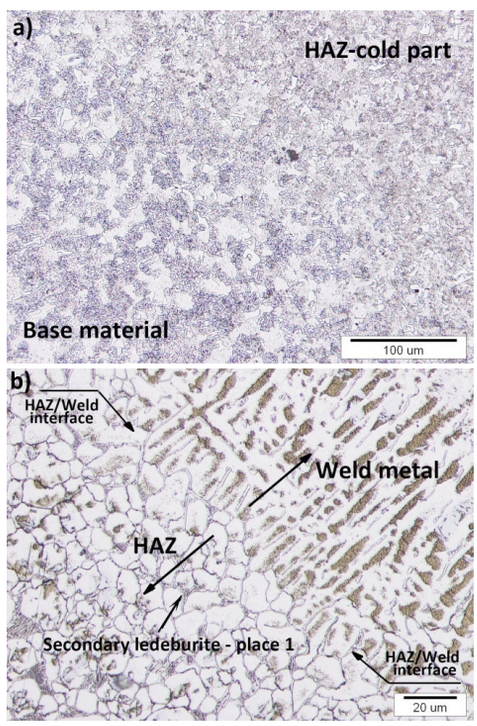

Figure 2. *Microstructure of the distinctive areas of weld joint (OM): a) base material/HAZ interface, b) HAZ/weld metal interface, (SAW technique, V-joint weld).*

weld, produced by SAW technique is shown in Fig. 4. The microstructure of the base material/HAZ–cold part interface is visible in Fig. 4a, while Fig. 4b shows an area of secondary ledeburite, with its typical lamellar structure. Larger secondary ledeburite areas were found only in HAZ-hot part. At the HAZ/weld metal interface, secondary ledeburite was formed only on the crystal grain boundaries in the HAZ (Fig. 4c). Fig. 5a shows a larger cluster of secondary ledeburite in the HAZ–hot part, with semi-quantitative line analysis across the matrix and secondary ledeburite cluster (Fig. 5b).

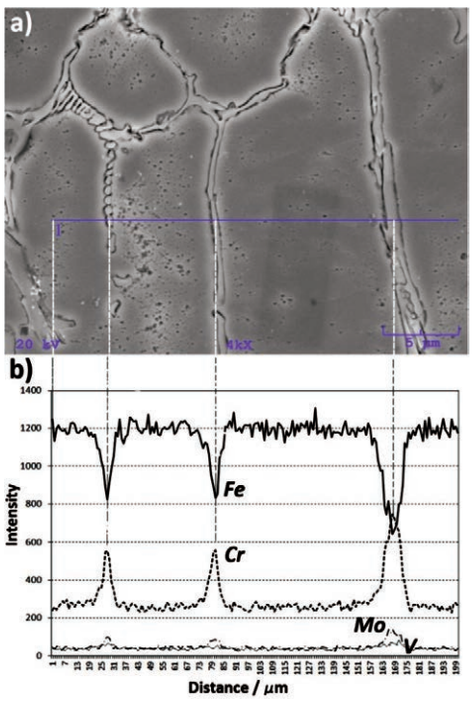

Figure 3. *a) HAZ - hot part microstructure: secondary ledeburite at the matrix grain boundaries (SEM), b) the concentration profile (EDXS semi-quantitative line analysis),(SAW technique, V-joint).*

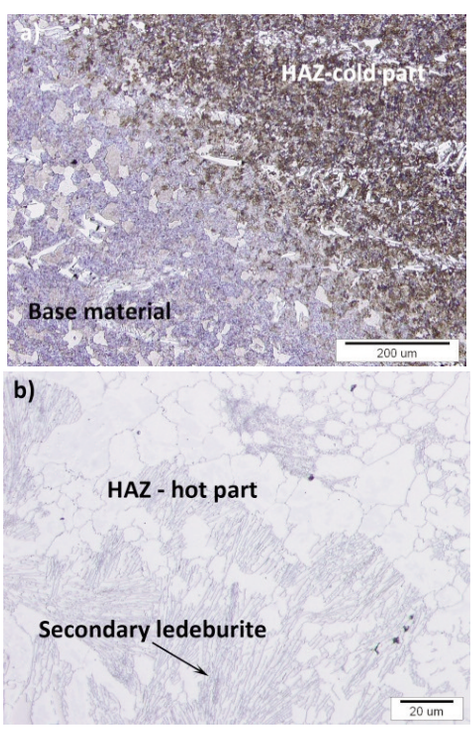

Figure 4. *Microstructure of the surface weld at the distinctive areas (OM), a) base material/HAZ interface, b) HAZ – hot part, c) HAZ/weld metal interface, (SAW technique).*

Microstructure of distinctive areas of surface weld, produced by the TIG surfacing technique is shown in Fig. 6 and with a detail analysis of partially dissolved primary carbide in Fig. 7. The average HAZ width was 1 mm. Similar to the SAW technique, areas of partially or completely dissolved primary carbides were found in the hot part of HAZ, which caused subsequent secondary ledeburite formation.

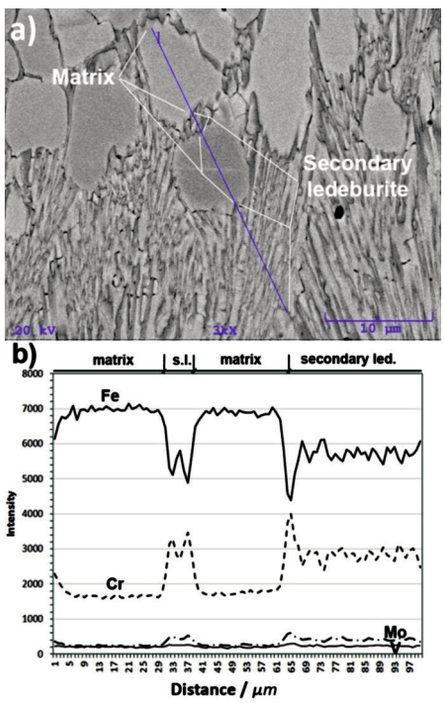

Figure 5. *a) Microstructure of the HAZ-hot part (SEM),b) the concentration profile of alloying elements across the matrix grain and secondary ledeburite, (SAW surfacing technique).*

Fig. 8a shows the microstructure of the base material/HAZ interface, while Fig. 8b shows the microstructure in the hot part of HAZ near the HAZ/weld metal interface, after surfacing with the microplasma technique. The specific distribution of iron, chromium and manganese around partially dissolved primary carbide is shown in Fig. 9. The average HAZ width was 0,9 mm.

Fig. 10 shows the microstructure of a specimen after the surface laser welding technique. On the base material/weld metal interface (Fig. 10b), broken, partially dissolved primary carbides can be seen. In this case the dissolution of carbides and melting of their surrounding helped to fill the cracks (Fig. 10b).

Chemical composition of undissolved primary carbide, matrix of the base material, and the area between the segments of cracked, partially dissolved carbide are presented in Table 3. Specific element distribution (mapping) of partially dissolved primary

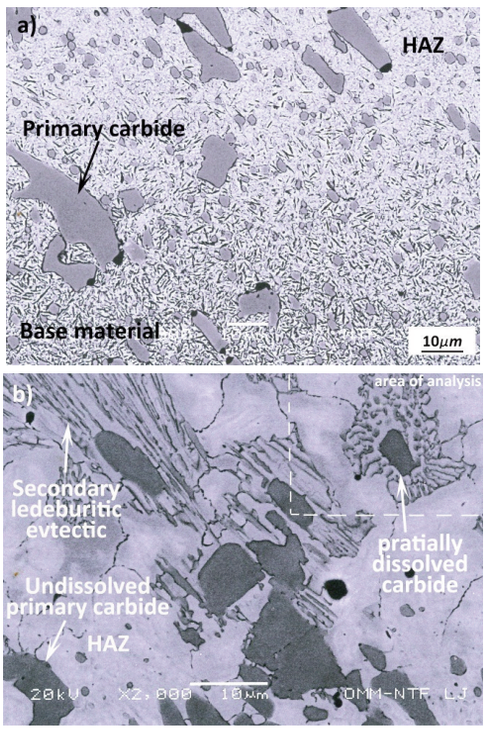

Figure 6. *Microstructure of distinctive areas in the surface weld (SEM): a) base material/HAZ interface, b) HAZ –fusion zone, (TIG surfacing technique).*

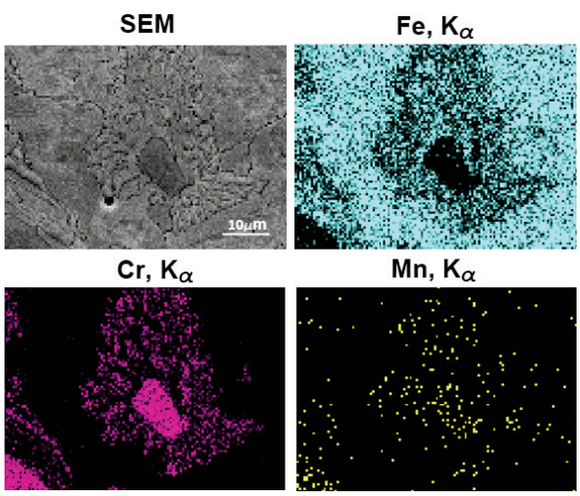

Figure 7. *SEM micrograph and specific X-ray distribution (mapping) of iron, chromium and manganese in the area of partially dissolved primary carbide and in the secondary ledeburite in the HAZ-hot part, (TIG surfacing technique).*

carbide is shown in Fig. 11a. Besides chromium, carbides contain iron, vanadium, molybdenum and manganese. EDXS line semi-quantitative analysis revealed that dissolution of carbide is a consequence of mostly chromium diffusion into the matrix (Fig.11c). Due to extremely narrow heat penetration

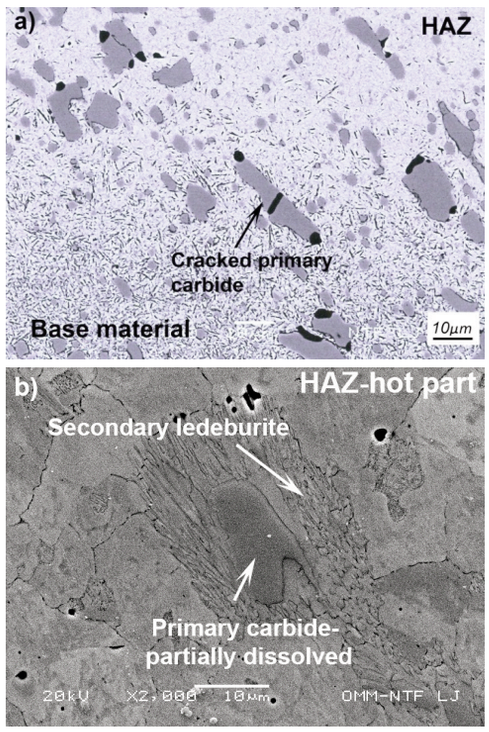

Figure 8. *Microstructure of distinctive areas of the surface weld (SEM): a) microstructure of the base material/HAZ interface, b) microstructure of the HAZ – hot part, partially dissolved primary carbide surrounded by secondary ledeburite, (microplasma surfacing technique).*

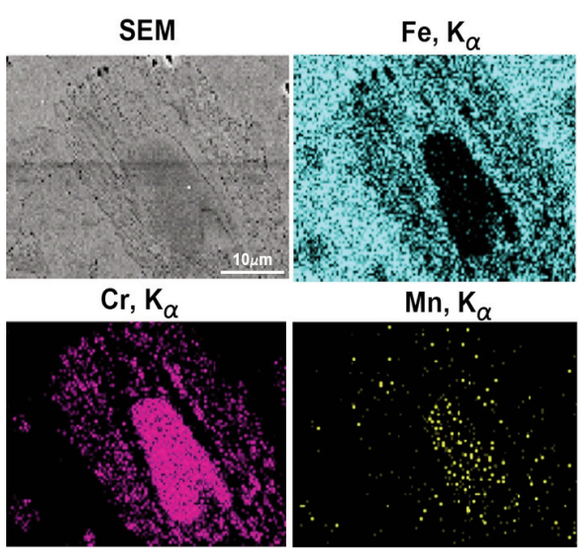

Figure 9. *SEM micrograph and specific X-ray distribution (mapping) of iron, chromium and manganese in the area of partially dissolved primary carbide and in the secondary ledeburite in the HAZ-hot part, (microplasma surfacing technique).*

area and high cooling rate, the heat affected zone is very narrow and undeveloped.

Table 3. *Chemical composition (without carbon) of microstructural constituents (laser surfacing).*

Place of analysis	Chemical composition / wt.%				
	Fe	Mn	Cr	V	Mo
Primary carbide (position [1], Fig. 10a)	43.5	0.34	47.9	6.6	1.7
Matrix in the base material (position [2], Fig. 10a)	91.7	0.16	7.1	0.46	0.6
Matrix between the segments of primary carbide (position [2], Fig. 10b)	75	/	20.8	2.4	1.6

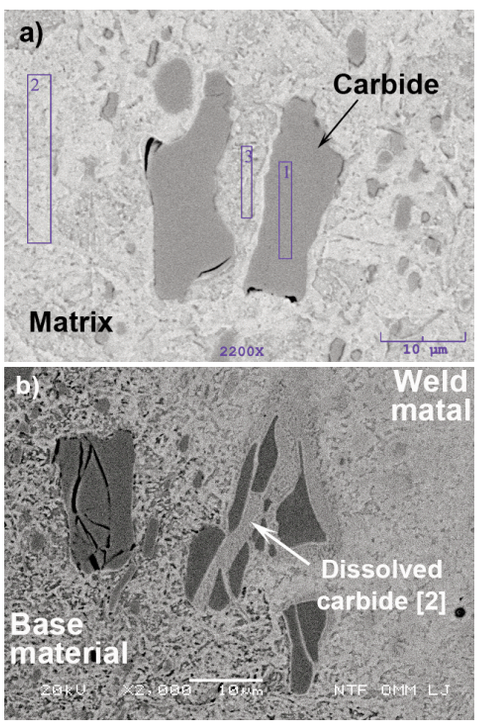

Figure 10. *Microstructure of distinctive areas of surface weld (SEM): a) microstructure of the base material, b) microstructure of the base material/weld metal interface, (laser surfacing).*

Sequence of the phase transformations of the examined steel during heating (10K/min) was followed by DTA method. DTA heating curves of forged (as processed, without heat treatment) and cast sample are shown in Fig.12. Cast sample was prepared by remelting and slow cooling of forged sample, cut off from the same forged bulk piece.

According to the calculated phase diagram [14], the distinctive peaks of the DTA heating curves could be interpreted as follows: The first peak (exothermic) corresponds to decomposition of martensite into ferrite and carbides (tempered martensite). Wider temperature interval, lower temperature of the

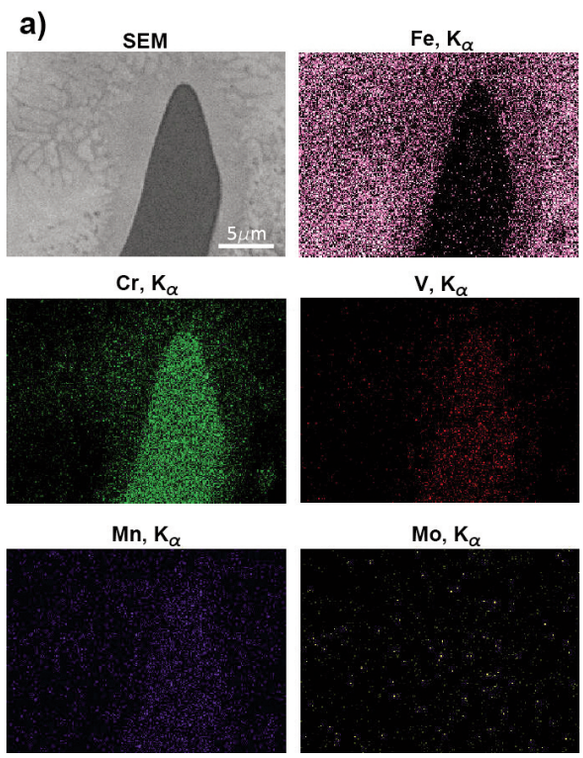

Figure 11. *a) Microstructure (SEM) and specific X-ray element distribution (mapping) of partially dissolved primary carbide (base material/weld metal interface), b) area of partially dissolved primary carbide (SEM), c) the concentration profile of alloying elements across the matrix/carbide boundary, (laser surfacing).*

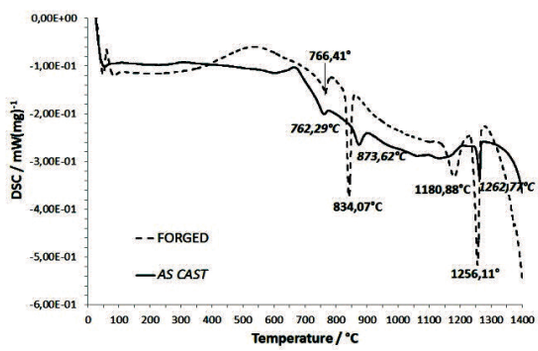

Figure 12. *DTA heating curves of W.nr. 1.2379 tool steel in as cast and forged state.*

maximum transformation rate (T_{p1f} = 534 °C) and higher energy of the peak are connected with the larger amount of martensite in the forged sample, compared to remelted one (T_{p1c} = 664 °C). The reader should be aware, that this steel has very good hardenability (air hardenable). Peak 1 on remelted sample DTA heating curve indicates that cooling rate was not sufficiently slow to completely prevent

martensite formation. The second peak (T_{p2f} = 766 °C and T_{p2c} = 762 °C) corresponds to the maximum dissolution rate of secondary carbides $M_{23}C_6$ in the matrix. Austenitization begins within a temperature interval with distinctive peak 3 (T_{p3f} = 834 °C and T_{p3c} = 873 °C). Higher energy required and lower temperature of transformation is connected to the larger amount of retained austenite and carbide distribution in forged sample. Peak 4 (T_{p4f} = 1180 °C) was detected only in forged sample and corresponds to ternary eutectic (γ_{Fe} + $M_{23}C_6$ + M_7C_3) decomposition. The absence of peak 4 on remelted sample DTA heating curve indicates that this is a metastable eutectic. It should be noted, that this eutectic was not detected by other researchers [15], which leads us to the conclusion, that occurrence of this eutectic is a consequence of irregular production parameters (wrong temperature ramping or insufficient soaking time before forging). Peak 5 (T_{p5f} = 1256 °C and T_{p5c} = 1262 °C) correspond to decomposition of primary ledeburite (γ_{Fe} + M_7C_3) and dissolution of M_7C_3 carbides. Austenite matrix began to melt at temperatures above 1390 °C.

4. Discussion

In all applied welding techniques, with the exception of laser welding method, the conditions for the formation of secondary ledeburite were met, i.e. adequate temperature and time to melt the matrix in the vicinity of primary carbides. The sequence of secondary ledeburite formation can be explained through the occurrence of intermediate transformation stages of primary carbides decomposition, detected in the microstructure after welding with various welding techniques. Fig. 13a shows a microstructure with unaffected primary carbide in the base material. It should be noted that such primary carbides are formed through the process of eutectic carbide coarsening and behave in the similar manner as eutectics. Their melting temperature (Fig. 12, ≈1260°C) is practically the same as for eutectics in as cast state. In the heat affected zone, cracking of larger primary carbides

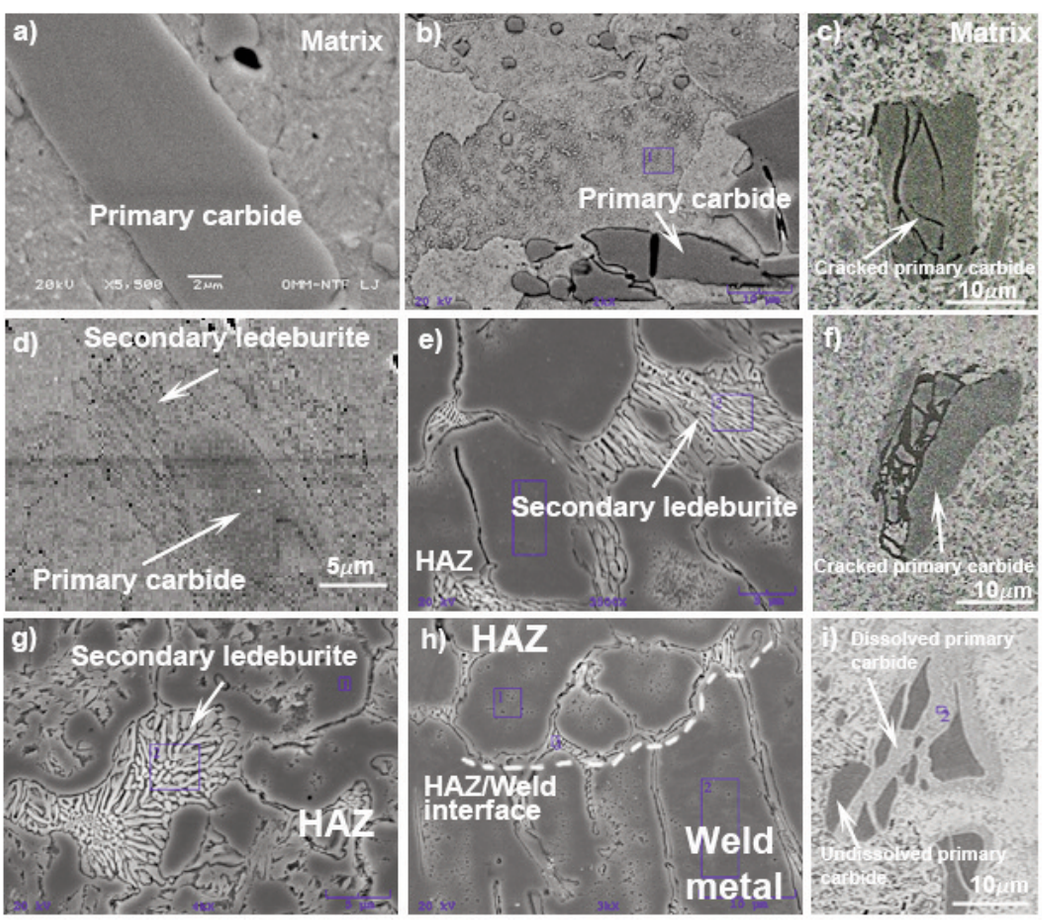

Figure 13. *Microstructure of base material and heat affected zone (SEM): a) primary carbide in the base material, b;c;f) broken primary carbides in the cold part of HAZ, d;e;g) secondary ledeburite next to partially dissolved primary carbides, h) secondary eutectic on the HAZ/weld interface, i) partially dissolved fragments of primary carbide.*

occur during welding, due to thermal stresses (Fig. 13b, c, f). In the hot part of HAZ the dissolution of primary carbide particles starts. Containment of low temperature melting ternary eutectic only promotes the dissolution of primary carbides. The dissolution rate is strongly temperature dependant, and can be very fast at high temperatures, even when the duration of exposure to high temperature is extremely short (Fig. 13i, laser welding). Dissolution of carbides increases the content of chromium, carbon and other alloying elements in the matrix to the extent of eutectical composition, which will locally melt, if the actual temperature in that area exceeds the melting temperature of the eutectic. During cooling, this melt solidifies as secondary lamellar ledeburite (Fig. 13d, e, g). The size of the secondary ledeburite area and the size of individual carbide lamella increases with actual temperature in the region and decreasing cooling rate, respectively (Fig. 13e, g). Due to constitutional undercooling in the fusion zone and weld metal bead, filler metal solidifies ahead of solidification front and capture the eutectic melt at the HAZ/weld metal interface (Fig. 13h, welded with SAW technique). Depending on the degree of the constitutional undercooling, the solidification structure changes from columnar to globular (Fig. 14). Welding techniques with a wider heat affected zone and deeper filler material penetration (SAW, TIG) are more prone to the formation of secondary ledeburitic net around the matrix crystal grains.

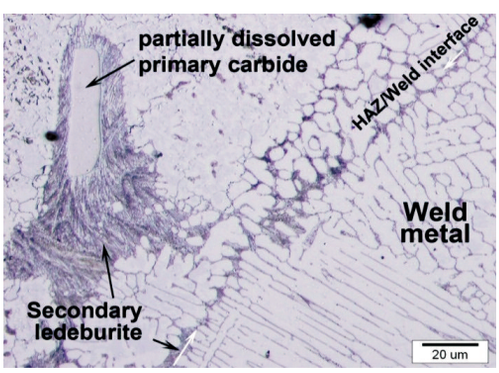

Figure 14. *Partially dissolved primary carbide surrounded by secondary ledeburite; secondary ledeburite at the HAZ/Weld metal interface, (OM, SAW technique).*

5. Conclusions

The present paper describes changes in the heat affected zone of tool steel W.N.1.2379, which was welded by SAW, TIG, laser and microplasma methods. The purpose of this research was to determine the microstructure transformations after various welding techniques, especially in the heat affected zone with the accentuation on the primary/eutectic carbides behaviour during welding. We came to the conclusion that the formation of secondary ledeburite is a result of local remelting of enriched matrix with alloying elements, due to partial or complete dissolution of larger primary carbides. The amount of its occurrence depends on the actual temperature in the heat affected zone. The fact, that dissolution of larger primary carbide was also detected after laser welding technique, gives as a proof that the carbide dissolution rate is extremely fast at high temperature. A small amount of homogeneously distributed low temperature melting ternary eutectic probably don't affect mechanical properties, but special care should be paid to avoid their occurrence, when subsequent welding will be applied, because they promote the formation of secondary ledeburite. The results show that the largest amount of secondary ledeburite is formed during submerged arc welding, followed by TIG and microplasma welding technique, which is closely linked with their heat affected zone width and the amount of heat energy input. The formation of secondary ledeburite was not detected when laser surfacing technique with appropriate technological parameters was applied.

References

[1] Z. H. Wang, Q. B.Wang, L. Cui, A. D. Yang, D. Y. He, Sci. and Technol. Weld. Joining, 13 (2008) 656-662.

[2] G. F. Vander Voort, Buehler Ltd, Metallographic Techniques for Tool Steels, (2004)

[3] N. Yasavol, A. Abdollah-Zadeh, D. M. Rodrigues, Proceedings of the second international conference, Friction Stir Welding and Processing, (2012), 51-53.

[4] J. Zachrisson, J. Borjesson, L. Karlsson, Sci. and Technol. Weld. Joining, **7** (2013) 603-609.

[5] M. Filipović, Ž. Kamberović, M. Korać, J. Min. Metall, 50 (1) B (2014) 27-30.

[6] P. Podržaj, S. Simončič, Sci. and Technol. Weld. Joining, 18 (2013) 551-557.

[7] M. P. Tonkovič, L. Kosec, Metallurgy, 49 (2010) 155-160.

[8] H. Gao, M.J.M. Hermans, I.M. Richardson, Sci. and Technol. Weld. Joinin, 18 (2013) 525-531.

[9] H. Gaul, G. Weber, M, Rethmeier, Sci. and Technol. Weld. Joining, 16 (2011) 440-445.

[10] J. V. Tuma, G. Kosec. Steel Research International, 78 (2007) 643-647.

[11] B. Hanhold, S. S. Babu, G. Cola, Sci. and Technol. Weld. Joining, 18 (2013) 253-260.

[12] R. Celin, J. Tušek, D. Kmetič, J. V. Tuma, Materials and Technologies, 35 (2001) 405-408.

[13] G. Kosec, A. Nagode, I. Budak, A. Antić, B. Kosec, Engineering Failure Analysis, 18 (2011) 450-454.

[14] http://www.calphad.com/martensitic_stainless_steel_for_knives_part_2.html

[15] M. Gojić, B. Mioć, L. Kosec, Kovové Materiály, 44 (2006) 119-126.